Ab initio calculation of the radiative lifetimes of the $^1\Sigma^+$ and $^1\Pi$ excited states of CuCl

A. Ramírez-Solís and J. P. Daudey
Laboratoire de Physique Quantique, Université Paul Sabatier, 118, route de Narbonne, 31062 Toulouse CEDEX, France
(Received 22 May 1990)

Multiconfiguration self-consistent-field followed by multireference-configuration-interaction calculations using localized molecular orbitals were performed to obtain zeroth- and first-order perturbed Möller-Plesset (MP) wave functions and transition dipole moments for the $X\,^1\Sigma^+$ (ground), $^1\Sigma^+$, and $^1\Pi$ states to calculate the radiative lifetimes of these excited states. In order to improve the quality of the transition dipole moment between the initial and final states using orthogonal basis sets, an alternative approach based on state-averaged $\bar{G}^{(0)}$ and $\bar{G}^{(1)}$ (zeroth-order and MP perturbed) spinless one-particle reduced matrices to obtain mean adapted orbitals (MAO's) is proposed. This method is tested on the spin-allowed $X\,^1\Sigma^+ \leftarrow {}^1\Sigma^+, {}^1\Pi$ transitions, where excellent agreement with the experimental lifetimes is obtained. It was found that the difference in convergence, as far as the transition dipole moments are concerned, when using the MAO's obtained through $\bar{G}^{(0)}$ or $\bar{G}^{(1)}$ is very small, and therefore the additional effort to obtain the first-order MAO's is no longer justified.

I. INTRODUCTION

There has been recent work, both theoretical[1–7] and experimental,[8–12] on the spectroscopy of the CuX (X being a halogen atom) family. These molecules are interesting from the practical (used as chemical lasers) and also from the theoretical point of view, since copper halides show fairly complicated optical spectra and the heavier the halide, the more fragmentary and complicated these spectra become. The chemiluminescent spectroscopy of these molecules has been used to study the dynamics of reactive collisions of the type[13,14]

$$M + X_2 \rightarrow MX + X \ ,$$

where the presence of numerous interacting potential-energy surfaces raises interesting fundamental questions.

In particular, the accurate measurements of Steele and Broida[15] of some of the first excited states of CuF allowed Delaval *et al.*[11] to assess the nature (singlet or triplet) of the lowest excited states of CuCl by comparing the corresponding radiative lifetimes.

Delaval and Schamps[3] were the first to attempt (successfully) a theoretical estimation of the radiative lifetimes on a CuX molecule (CuF) through a spin-orbit-perturbed *ab initio* self-consistent-field (SCF) single-reference configuration-interaction (CI) calculation. In their work they showed that the simple picture $Cu^+(3d^9 4s^1)F^-(p^6) \rightarrow Cu^+(3d^{10})F^-(p^6)$ (atomically forbidden) to explain the observed transitions from the first excited to the ground state of CuF is completely wrong if one considers only the molecular polarization of the atomic copper orbitals. Since in the present work we are only interested in the first spin-allowed electronic transitions to the $X\,^1\Sigma^+$ ground state of the CuCl molecule we perform accurate multireference CI calculations to obtain reliable enough wave functions, energy differences, and transition dipole moments for the first singlet excited states, namely, the $^1\Sigma^+$ and $^1\Pi$ ones, to calculate their respective radiative lifetimes.

In Sec. II we explain the procedure used to calculate accurate transition energies using the multiconfiguration self-consistent-field (MCSCF) adapted orbitals for each state as building blocks for their respective multireference configuration-interaction (MRCI) wave functions. In Sec. III we shall briefly recall the fundamentals underlying the calculation of radiative lifetimes and the simplifications we can make in our particular case. In Sec. IV we present the results and discuss some of the difficulties one encounters when calculating accurate transition dipole moments between two states belonging to the same molecular symmetry. We suggest a method to obtain a set of mean natural orbitals which describe, with approximately the same quality, both states. Finally in Sec. V we give the general conclusion.

II. METHOD

We have used a double strategy in order to obtain the two basic quantities (transition energies and transition dipole moments) needed to calculate radiative lifetimes. First we performed MCSCF plus MRCI calculations to accurately evaluate the transition energies and equilibrium geometries of the $^1\Sigma^+$ and $^1\Pi$ excited states as well as the $X\,^1\Sigma^+$ ground state. Second, in order to overcome the difficulty of nonorthogonal basis sets, we have calculated the transition dipole moments between these excited states and the ground state at the SCF plus MRCI level using the common set of canonical molecular orbitals (MO's) of the latter.

This mixed approach is justified by the fact that the transition energies calculated using the SCF MO's of the ground state are largely overestimated (see Table I) and thus an optimization of the MO's corresponding to the excited states must imperatively be performed via an MCSCF calculation for each state.

TABLE I. SCF+MRCI transition energies, equilibrium geometries, and harmonic frequencies using the canonical MO's of the $X\,^1\Sigma$ ground state for all the states. Mean perturbational norm was 0.12.

State	T_e (cm^{-1})	R_e (a_0)	ω_e (cm^{-1})
$X\,^1\Sigma^+$	0	4.01	339
$^1\Pi$	28 567	4.04	328
$^1\Sigma^+$	24 576	4.07	402

A. Computational details

Self-consistent-field followed by localized multiconfiguration SCF and multireference-configuration-interaction (LMCSCF-MRCI) calculations are performed for the $X\,^1\Sigma^+$ (ground) and $^1\Sigma^+$, $^1\Pi$ excited states of the CuCl molecule neglecting the spin-orbit term in the electronic Hamiltonian.

The relativistic effective core pseudopotential (RECP) method of Durand and Barthelat[16] is used to describe the core electrons of Cu and Cl. Thus for the copper atom we have an argon-type core and treat explicitly only the 11 valence electrons ($d^{10}s^1$) while for the halogen we are left with a neon-type core and 7 valence electrons (s^2p^5). These pseudopotentials include all the relativistic effects except the spin-orbit effect.

The pseudopotential for copper is taken from Ref. 17 along with the Gaussian basis set which is of triple-ζ quality for the $3d$ and $4s$ shells and of double-ζ quality for the $4p$ polarization function. The chlorine pseudopotential parameters and basis set can be found in Refs. 18 and 7, respectively. The basis set used is of quadruple-ζ quality for the $3s$ and $3p$ shells and has a single-ζ $3d$ polarization function optimized to reproduce at best the experimental atomic $^4P \rightarrow {}^2P$ and $^2P \rightarrow {}^2P$ transition energies.

Since it is well known that the first excited states of CuCl arise directly as a consequence of the excitation of the Cu^+ ion in its $^1S(d^{10})$ ground state to the $^3D(d^9s^1)$ and $^1D(d^9s^1)$ states, we evaluated[7] the lower part of the atomic spectra of Cu and Cu^+; results are found to be in good agreement with experimental data.

B. Localization of the molecular orbitals

In order to properly account for the nondynamical correlation energy we used our localization algorithm reported in Ref. 6 in exactly the same way it was used to deal with CuF.

C. Multiconfiguration self-consistent-field

It is known[7] that the use of the SCF orbitals of the $X\,^1\Sigma^+$ ground state to describe the first excited states of CuCl leads to largely overestimated transition energies and underestimated vibrational frequencies. One is therefore forced to perform an MCSCF calculation for each of the excited states one is interested in, to obtain a reasonable set of orbitals to be used as the monoelectronic basis in a multireference CI calculation for each excited state.

Before localization, the main configurations of the states we are dealing with are

$$X\,^1\Sigma^+\text{: } 9\sigma^2 10\sigma^2 4\pi^4 1\delta^4 5\pi^4 11\sigma^2 ,$$

$$^1\Pi\text{: } 9\sigma^2 10\sigma^2 4\pi^3 1\delta^4 5\pi^4 11\sigma^2 12\sigma^1 ,$$

$$^1\Sigma^+\text{: } 9\sigma^2 10\sigma^2 4\pi^4 1\delta^4 5\pi^4 11\sigma^1 12\sigma^1 .$$

It should be said that an MCSCF description of the excited states including all the possible configuration state functions (CSF's) generated by the active orbitals found to play a predominant role, namely, the 11σ, 12σ, and 4π (the complete active space SCF generated by six electrons on four active orbitals), leads to much smaller transition energies than experimental ones, while harmonic vibrational frequencies and equilibrium distances are too large compared with experimental data.[7]

We have included up to ten of the most important configurations describing both excited states, although only two or three of them actually have an important effect in the orbital optimization.

D. Multireference configuration interaction

The MRCI calculations were performed with the configuration interaction and perturbation through selected iterations (CIPSI) algorithm[19] in its two-class version where a small reference space (S) is used as a generator of perturbed determinants (P space) interacting with those in S [in the Möller-Plesset (MP) partition of the electronic Hamiltonian] up to second order. In practice the number of determinants that are to be included in the reference space S is determined for each state, so as to have perturbational norms (within the intermediate normalization) of similar magnitude for all states. Of course there always exists some uncertainty as to the relative quality of the wave functions for different states, but this norm is used as a criterion to keep approximately the same ratio of perturbational to variational contributions to the total energy for all three states. It was kept between 0.08 and 0.10. Table II shows the sizes of the variational and perturbational spaces for each state as well as the corresponding norms.

Let $|\psi_K^{(0)}\rangle$ represent the zeroth-order wave function of state K and $|\psi_K^{(1)}\rangle$ the first-order perturbational part of this state. The total wave functions of states K and L are given by

$$|\psi_K\rangle = |\psi_K^{(0)}\rangle + |\psi_K^{(1)}\rangle = \sum_{n\in S} C_K^n |\psi_n\rangle + \sum_{m\in P} C_K^m |\psi_m\rangle , \quad (1)$$

$$|\psi_L\rangle = |\psi_L^{0}\rangle + |\psi_L^{(1)}\rangle = \sum_{n'\in S} C_K^{n'} |\psi_{n'}\rangle + \sum_{m'\in P} C_K^{m'} |\psi_{m'}\rangle . \quad (2)$$

TABLE II. Number of determinants in the reference (S) and perturbational P spaces and their respective norms.

State	Size of S	Size of P	Norm
$X\,^1\Sigma^+$	128	4×10^6	0.078
$^1\Pi$	400	11.3×10^6	0.080
$^1\Sigma^-$	494	14×10^6	0.096

III. RADIATIVE LIFETIMES

We shall be concerned with electronic state lifetimes in the remainder of the paper. We will consider only the electric dipole approximation to deal with radiative transitions and neglect higher-order electric multipoles and the magnetic dipole contribution since they are much smaller (by a factor ranging from 10^{-7} to 10^{-8}) than electric dipole moments.

Since the (increasing) energetic ordering of the lowest electronic states is[7] $X\,^1\Sigma^+$, $^3\Sigma^+$, $^3\Pi$, $^1\Pi$, $^1\Sigma^+$, $^3\Delta$, $^1\Delta$, the only dipole allowed transitions within the Born-Oppenheimer approximation towards the ground state are the $X\,^1\Sigma^+ \leftarrow {}^1\Sigma^+$ and $X\,^1\Sigma^+ \leftarrow {}^1\Pi$ transitions. A cascading process is therefore possible only for the $^1\Sigma^+$ state, which could temporarily decay into the $^1\Pi$ excited state and finally to the ground $X\,^1\Sigma^+$ state.

The transition probability of a given (Λ',Σ',v',J') rovibronic state is given by

$$\tau^{-1}_{\Lambda'\Sigma'v'J'} = \sum_{\Lambda''}\sum_{\Sigma''}\sum_{v''}\sum_{J''} A_{\Lambda'\Sigma'v'J',\Lambda''\Sigma''v''J''} , \tag{3}$$

where the Einstein A coefficients are given in atomic units by

$$A_{\Lambda'\Sigma'v'J'\Lambda''\Sigma''v''J''} = \frac{32\pi^3}{3c^3}\nu^3_{\Lambda'\Sigma'v'J'\Lambda''\Sigma''v''J''}\frac{q_{v'v''}}{(2J'+1)} \times |\langle \psi_{\Lambda''\Sigma''}|\boldsymbol{\mu}|\psi_{\Lambda'\Sigma'}\rangle|^2 \tag{4}$$

and $q_{v'v''}$ is the vibrational Franck-Condon factor. The frequency $\nu_{\Lambda'\Sigma'v'J'\Lambda''\Sigma''J''}$ can be divided into three contributions:

$$\nu_{\Lambda'\Sigma'v'J'L''\Sigma''v''J''} = (T'_e - T''_e) + [G'(v') - G''(v'')] + [F'(J') - F''(J'')] , \tag{5}$$

with $\Delta J = 0, \pm 1$. The rotational energy differences involved in CuCl are of the order of 0.4 cm^{-1} (Ref. 10), which is completely negligible compared with $(T'_e - T''_e)$ ($> 13\,000$ cm^{-1}). Moreover, since the upper and lower potential-energy curves are nearly parallel, having approximately the same equilibrium distances and vibrational frequencies, the vibrational intensity is mostly confined within the principal sequence $\Delta v = 0$; we can safely approximate the Franck-Condon factor $q_{v'v''}$ as

$$q_{v'v''} = \delta_{v'v''} .$$

We can then write the transition probability as

$$\tau^{-1}_{\Lambda'\Sigma'v'J'} = \sum_{\Lambda''}\sum_{\Sigma''}\frac{32\pi^3}{3c^3} g_e (T'_e - T''_e)^3 |\langle \psi_{\Lambda''\Sigma''}|\boldsymbol{\mu}|\psi_{\Lambda'\Sigma'}\rangle|^2 , \tag{6}$$

where g_e is a statistical factor equal to unity except for the $\Sigma \rightarrow \Pi$ transition where $g_e = 2$. We shall be interested to compare our results with the experimental data of Delaval *et al.*[11] obtained through resonance fluorescence and collision-induced fluorescence. This means that only transitions between states of the same spin multiplicity $\Sigma'' = \Sigma'$ will contribute to the total transition probability.

On the other hand, as Delaval and Schamps[3] have already pointed out for the radiative transitions in CuF, the transition probabilities between excited states are exceedingly small for two reasons. The first is that in the atomic limit $Cu(3d^{10}4s^1) + Cl(3s^23p^5)$ they correspond to forbidden transitions $\Delta l = 0$ ($3d \rightarrow 3d$). The second argument is a purely energetic one: since the molecular excited states lie so close, the $(T'_e - T''_e)^3$ factor is about 10^{-5} to 10^{-6} times smaller than the one corresponding to the transition towards the $X\,^1\Sigma^+$ ground state. Experimentally $T_e(^1\Sigma^+) - T_e(^1\pi) = 111$ cm^{-1}, to be compared with 23 000 cm^{-1} from the difference $T_e(^1\Sigma^+) - T_e(X\,^1\Sigma^+)$. For these reasons, the probability of cascading for the $^1\Sigma^+$ excited state ($^1\Sigma^+ \rightarrow {}^1\Pi \rightarrow X\,^1\Sigma^+$) is completely negligible.

So we end up with two simple expressions to evaluate the radiative lifetimes of the $^1\Sigma^+$ and $^1\Pi$ excited states:

$$\tau^{-1}_{^1\Sigma^+} = \frac{32\pi^3}{3c^3}\nu^3_{^1\Sigma^+, X\,^1\Sigma^+} |\langle {}^1\Sigma^+|\mu_z|X\,^1\Sigma^+\rangle|^2 , \tag{7}$$

$$\tau^{-1}_{^1\Pi} = \frac{32\pi^3}{3c^3}\nu^3_{^1\Pi, X\,^1\Sigma^+} |\langle {}^1\Pi|\mu_x + i\mu_y|X\,^1\Sigma^+\rangle|^2 . \tag{8}$$

IV. RESULTS AND DISCUSSION

Before the localization algorithm was applied to the SCF canonical MO's, three of the occupied orbitals were already localized: 9σ on chlorine $3s$, and 1δ on copper $3d_\delta$. The remaining six nonlocalized MO's can be grossly described as follows: the highest occupied MO (HOMO) 11σ is shared by the $3d$ atomic orbital (AO) on copper, the $3s$ and $3p$ ones on chlorine, while the lowest unoccupied MO (LUMO) 12σ was mainly located on copper $4s$ with an important polarization component on chlorine $3p$. The two highest occupied σ MO's, 10σ and 11σ, possess one nodal plane; the 4π and 5π orbitals are completely nonlocalized mixtures of the copper $3d_\pi$ and chlorine $3p_\pi$. The main configurations after localization can be translated to AO's as follows:

$$X\,^1\Sigma^+: \; Cu^+(3d_\delta^4 3d_\pi^4 3d_\sigma^2)Cl^-(3s^2 3p_\sigma^2 3p_\pi^4) ,$$

$$^1\Pi: \; Cu^+(3d_\delta^4 3d_\pi^3 3d_\sigma^2 4s^1)Cl^-(3s^2 3p_\sigma^2 3p_\pi^4) ,$$

$$^1\Sigma^+: \; Cu^+(3d_\delta^4 3d_\pi^4 3d_\sigma^1 4s^1)Cl^-(3s^2 3p_\sigma^2 3p_\pi^4) .$$

It is clear that the ionic $Cu^+(d^9s^1)Cl^-(s^2p^6)$ situation properly describes both excited states.

In Table III we present the calculated equilibrium and harmonic vibrational frequencies for the three states. It can be noted that equilibrium distances are between 0.09 and 0.2 bohr too long with respect to experimental data, and vibrational frequencies are somewhat smaller (10%)

TABLE III. Equilibrium geometries and harmonic vibrational frequencies. Experimental values in parentheses.

State	R_e (a_0)	ω_e (cm^{-1})
$X\,^1\Sigma^+$	3.97(3.88)	367(415)
$^1\Pi$	4.12(3.97)	368(393)
$^1\Sigma^-$	4.22(4.00)	341(403)

TABLE IV. MCSCF+MRCI transition energies to the $X\,^1\Sigma^+$ ground state in cm^{-1}.

State	Vertical	Exp.	Adiabatic
$^1\Pi$	22 980	22 959	23 226
$^1\Sigma^+$	20 558	23 070	21 267

than what they should be. We have carefully discussed both facts in Ref. 7. To remedy this, we proposed there to use the virtual atomic orbitals of the copper ion on its lowest (d^9s^1) configuration, namely, the ^3D spectroscopic term. This approach turned out to be the right one since, for the $X\,^1\Sigma^+$ ground state both spectroscopic constants were substantially improved: $R_e=3.93$ ($3.88a_0$) and $\omega_e=420$ (415 cm^{-1}). This proves that the first virtual MO's for these states slightly exaggerate the importance of the $Cu^+(d^{10})Cl^-(p^6)$ configuration with respect to the $Cu^+(d^9s^1)Cl^-(p^6)$ one.

Once the transition energies had been calculated we proceeded to evaluate the transition dipole moments.

Transition dipole moments

In order to evaluate transition dipole moments we used a single set of molecular orbitals to describe the three states and the fact that

$$\langle\psi_K|\hat{O}|\psi_L\rangle^{(i)}=\mathrm{Tr}(\hat{O}\Gamma^{(i)}_{K,L}),\quad i=0,1 \tag{9}$$

where $\hat{O}$ is the operator associated with the observable O and i stands for the perturbational order of the transition density matrix. Using Eqs. (1) and (2) we can write the zeroth- and first-order transition spinless one-particle density matrix in the common basis of orthogonal molecular orbitals (in second-quantized form) as follows:

$$\Gamma^{(0)}_{i,j}(K,L)=\langle\psi^{(0)}_K|\hat{a}^{\dagger}_i\hat{a}_j|\psi^{(0)}_L\rangle \tag{10}$$

and

$$\Gamma^{(1)}_{i,j}(K,L)=\langle\psi^{(0)}_K+\psi^{(1)}_K|\hat{a}^{\dagger}_i\hat{a}_j|\psi^{(0)}_L+\psi^{(1)}_L\rangle\ ,$$

where $\hat{a}^{\dagger}_i$ and its adjoint $\hat{a}_i$ are the electron creation and annihilation operators, respectively. We can make a further approximation to calculate the first-order transition density matrix and write it as

$$\begin{aligned}\Gamma^{(1)}_{i,j}(K,L)&\simeq\langle\psi^{(0)}_K|\hat{a}^{\dagger}_i\hat{a}_j|\psi^{(0)}_L\rangle+\langle\psi^{(0)}_K|\hat{a}^{\dagger}_i\hat{a}_j|\psi^{(1)}_L\rangle\\&\quad+\langle\psi^{(1)}_K|\hat{a}^{\dagger}_i\hat{a}_j|\psi^{(0)}_L\rangle\\&=\Gamma^{(0)}_{i,j}(K,L)+\langle\psi^{(0)}_K|\hat{a}^{\dagger}_i\hat{a}_j|\psi^{(1)}_L\rangle\\&\quad+\langle\psi^{(1)}_K|\hat{a}^{\dagger}_i\hat{a}_j|\psi^{(0)}_L\rangle\ ,\end{aligned} \tag{11}$$

where we have dropped the second-order terms

$$\langle\psi^{(1)}_K|\hat{a}^{\dagger}_i\hat{a}_j|\psi^{(1)}_L\rangle\ . \tag{12}$$

The reason behind this approximation is that the correction brought in by (12) to (11) is much too small compared with the first three terms in Eq. (11) and that the number of terms to be calculated is too time-consuming ($\sim10^7\times10^7$) to be worthwhile. In matrix notation the transition dipole moment between states K and L can be read as

$$\langle\psi_K|\boldsymbol{\mu}|\psi_L\rangle^{(i)}=\mathrm{Tr}(\boldsymbol{\mu}\Gamma^{(i)}_{K,L}),\quad i=0,1 \tag{13}$$

where $\boldsymbol{\mu}=\sum_i^{N_v}e\mathbf{r}_i$ and N_v stands for the number of valence electrons.

For simplicity, we chose to work with the SCF MO's of the ground state. Table I shows the calculated equilibrium geometries and harmonic frequencies for the three states we are interested in. The equilibrium distances are only 0.03 bohr apart. We can calculate the transition dipole moments for both excited states at the equilibrium distance of each one using this common MO basis; the physical implication behind this hypothesis is that the MO's involved in the electron jump describing the change of state will not differ much from the final MO's, namely, those of the ground state. As we will see, this proved to be an excellent approximation in the case of the $X\,^1\Sigma^+\leftarrow{}^1\Pi$ transition where the highest occupied d orbital (σ bond) is not much changed by the polarization induced when the $4s$ electron is transferred towards the

TABLE V. Transition dipole moments (in a.u.) and radiative lifetimes of the $^1\Pi$ and $^1\Sigma^+$ excited states using the canonical SCF MO's of the $X\,^1\Sigma^+$ ground state at their respective equilibrium geometries.

Initial state $\lvert i\rangle$	Perturbation order m	Number of determinants	$\langle X\,^1\Sigma^+\lvert\boldsymbol{\mu}\rvert i\rangle^{(m)}$	$\tau(\lvert i\rangle)$ (μsec)	Expt. Ref. 11
$\lvert^1\Pi\rangle$	0	in S $\begin{cases}X\,^1\Sigma^+\text{: } 270\\ ^1\Pi\text{: } 244\end{cases}$	$0.3515\hat{\imath}$	0.33	
$\lvert^1\Pi\rangle$	1	in P $\begin{cases}X\,^1\Sigma^+\text{: } 6\times10^6\\ ^1\Pi\text{: } 7\times10^6\end{cases}$	$0.3993\hat{\imath}$	0.26	0.45
$\lvert^1\Sigma^+\rangle$	0	in S $\begin{cases}X\,^1\Sigma^+\text{: } 270\\ ^1\Sigma^+\text{: } 513\end{cases}$	$0.0776\hat{k}$	9.42	
$\lvert^1\Sigma^+\rangle$	1	in P $\begin{cases}X\,^1\Sigma^+\text{: } 6\times10^6\\ ^1\Pi^+\text{: } 18\times10^6\end{cases}$	$-0.1204\hat{k}$	3.91	0.43

TABLE VI. Transition dipole moments (in a.u.) and radiative lifetimes using the zeroth- [MAO(0)] and first-order [MAO(1)] mean adapted orbitals for the $X\,^1\Sigma$ and $^1\Sigma^+$ excited state.

	Perturbational order m	Number of determinants	$\langle X\,^1\Sigma^+\|\mu\|^1\Sigma^+\rangle^{(m)}$	$\tau(^1\Sigma^+)$ (μsec)	(Expt.) 0.43	CPU μVAX (h)
MAO(0)	0	in S $\begin{cases} X\,^1\Sigma^+: & 436 \\ ^1\Sigma^+: & 538 \end{cases}$	$-0.3476\hat{k}$	0.469		0:03
	1	in P $\begin{cases} X\,^1\Sigma^+: & 10\times10^6 \\ ^1\Sigma^+: & 15\times10^6 \end{cases}$	$-0.3451\hat{k}$	0.473		4:00
MAO(1)	0	in S $\begin{cases} X\,^1\Sigma^+: & 603 \\ ^1\Sigma^+: & 691 \end{cases}$	$-0.3743\hat{k}$	0.405		14:00
	1	in P $\begin{cases} X\,^1\Sigma^+: & 14\times10^6 \\ ^1\Sigma: & 17\times10^6 \end{cases}$	$-0.3631\hat{k}$	0.430		18:00

$3d_\pi$ orbital of the ground state.

Using the calculated vertical transition energies appearing in Table IV, we give, in Table V the transition dipole moments and lifetimes of both excited states.

One can easily see that the canonical MO's of the $X\,^1\Sigma^+$ ground state are much better adapted to describe the $^1\Pi$ excited state than the $^1\Sigma^+$ one. This stems from the fact that the latter belongs to the same symmetry of the ground state and thus it is more difficult to properly describe it using the same set of MO's.

We would like to point out that, although small in absolute value, the transition dipole moment has the wrong sign (direction) between both Σ states, leading to a really inaccurate estimation of the corresponding lifetime; when we consider the first-order perturbed MP wave functions this is corrected and the new lifetime is significantly improved but still one order of magnitude too large (3.91 instead of 0.43 μsec).

On the other hand, the calculated lifetime for the $^1\Pi$ excited state even using the zeroth-order wave functions is quite close to the actual value. One would naturally ask why this value is slightly worse when considering the perturbed wave functions; we must remember that we used the MO's corresponding to the ground state. If one wants to really account for the actual process, we should have used the MO's corresponding to each electronic state, in this case the MCSCF MO's of the $^1\Pi$ state. However, this would mean working using nonorthogonal basis sets.

It is well known that, in order to describe monoelectronic properties such as dipole moments, the one-electron basis one uses should be of reasonable quality, even if a less-adapted MO basis can recover rather quickly a large portion of the correlation energy.

For this reason we propose here to obtain a mean set of adapted orbitals which describe, with approximately the same quality, both $^1\Sigma^+$ states. In order to do so, one can choose either the zeroth- or the first-order spinless one-particle density matrices of each state and then simply calculate their arithmetic mean as follows:

$$\bar{G}^{(i)}_{K,L} = \tfrac{1}{2}(\Gamma^{(i)}_{K,K} + \Gamma^{(i)}_{L,L}), \quad i = 0,1 \ . \tag{14}$$

It should be said that, with this notation, the bar over G applies only to the average of state (not transition) density matrices and the K,L subscripts simply tell us which states we have averaged. By diagonalizing these matrices one obtains a set of mean adapted orbitals (MAO's) that can be used to calculate the new wave functions [Eqs. (1) and (2)] $|\psi'_K\rangle, |\psi'_L\rangle$ and, with these, get an improved esti-

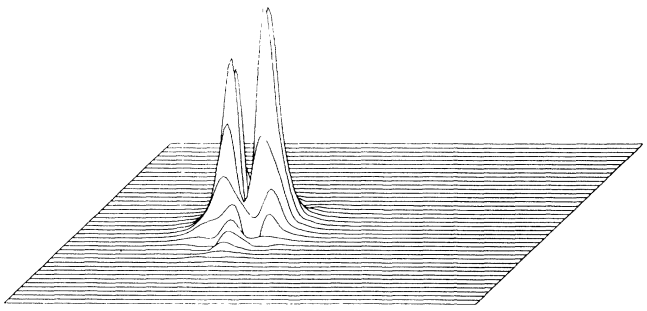

FIG. 1. X-Y plot of the electronic density of the HONO of the ground state. Occupation: $1.99e^-$.

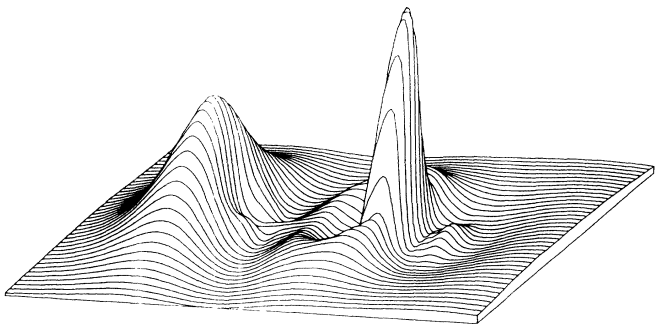

FIG. 2. X-Y plot of the electronic density of the lowest unoccupied natural orbital (LUNO) of the ground state. Occupation: $0.001e$.

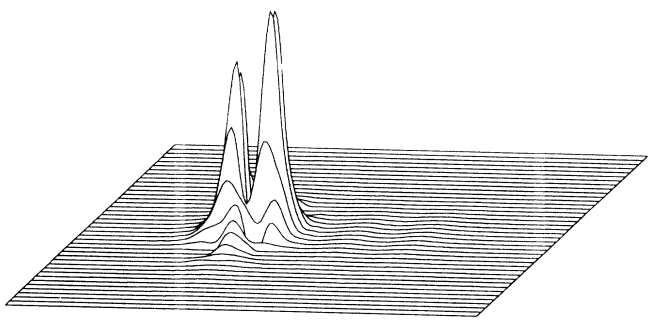

FIG. 3. X-Y plot of the electronic density of the second highest mean adapted orbital (MAO) between the ground state and the first Σ excited state. Occupation: $1.52e^-$.

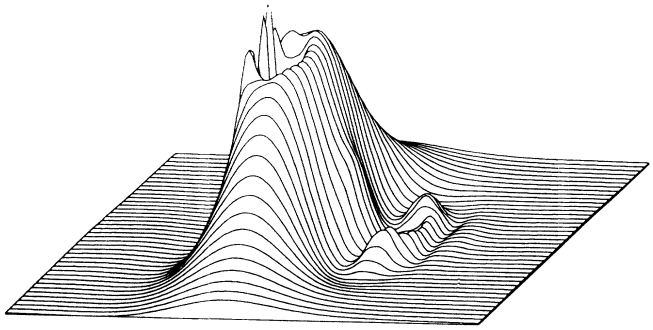

FIG. 5. X-Y plot of the electron density of the second highest occupied natural orbital of the first Σ excited state. Occupation: $1.22e^-$.

mate of the transition dipole moments using Eq. (13), either within the zeroth- or the first-order description of the transition density matrices.

It should be stressed here that the arithmetic mean of the density matrices [Eq. (14)] is only used as an intermediate to define the new set of adapted MO's and not as a real average density matrix with which we could calculate observables using Eq. (9).

In the upper part of the Table VI we present the result using the zeroth-order MAO's resulting from the diagonalization of $\bar{G}^{(0)}_{X\,^1\Sigma^+,\,^1\Sigma^+}$ at the equilibrium geometry of the $^1\Sigma^+$ excited state to calculate the zeroth- and first-order transition dipole moments and the corresponding radiative lifetimes. The lower part of this table shows the same results using the first-order MAO's. Two different comparisons can be made using Table VI. Firstly, note that the differences (using zeroth-order MAO's) between the zeroth- and first-order transition dipole moments is negligible (2×10^{-3} a.u.), thus leading to very small changes in the radiative lifetimes (4×10^{-4} μsec). The computer time required to obtain the perturbed transition dipole moment, once the variational wave functions had been calculated, was 4 h on a μVAX II as compared with 3 min using only the variational wave functions $|\psi^{(0)}_{X\,^1\Sigma^+}\rangle$ and $|\psi^{(0)}_{^1\Sigma^+}\rangle$. It is obvious that the computational effort is not worthwhile.

The second comparison concerns the transition dipole moments using the first-order MAO's. Their construction is a particularly time-consuming step since one must calculate twice ($\sim$7 h for each state) the spinless one-particle reduced density matrix using wave functions that contain approximately 10^7 determinants each; then the arithmetic mean of the density matrices and its diagonalization are readily performed. The values one obtains this way are not really very different from the ones calculated using the zeroth-order MAO's.

We can say that the only important differences in the occupation of the natural orbitals (NO's) of the $X\,^1\Sigma^+$ ground state and those of the $^1\Sigma^+$ excited state are found for the NO's corresponding (in the localized picture) mainly to the $3d_\sigma$ and $4s$ of copper. Their occupation in the ground (excited) state are 1.99 (1.22) and 0.001 (0.78) electrons, respectively, while the occupation of the corresponding mean adapted orbitals are 1.52 and 0.48 electrons. These values were obtained using the first-order density matrices but those calculated using the zeroth-order matrices are almost identical.

Some test calculations were made to see if the MAO's for the $X\,^1\Sigma^+$ and $^1\Pi$ states modified the already reasonable value of 0.33 μsec (experimental value was 0.45 μsec). The transition dipole moments obtained using the zeroth (first) -order MAO's are almost left unchanged: 0.3302 (0.3198 a.u.). These figures lead to a slight improvement of the radiative lifetime for the $^1\Pi$ state since we find 0.37 μsec (zeroth-order) and 0.39 μsec (first-order) to be compared with the experimental value of 0.45 μsec. These minor changes were to be expected because we

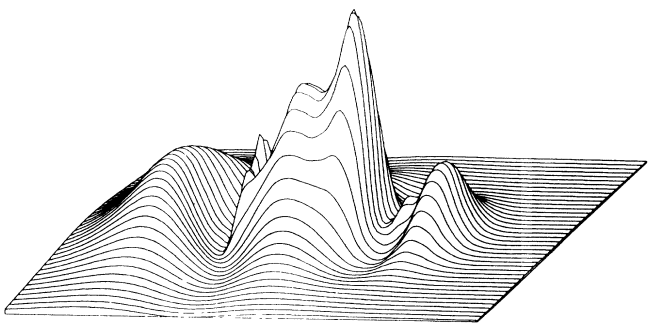

FIG. 4. X-Y plot of the electronic density of the highest occupied MAO. Occupation: $0.48e^-$.

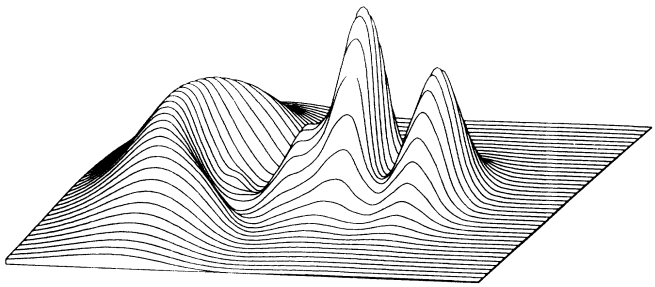

FIG. 6. X-Y plot of the electronic density of the highest occupied natural orbital of the Σ excited state. Occupation: $0.78e^-$.

knew that the orbitals involved in the electronic jump were already reasonably suited to describe both states for this transition.

Finally, for comparison purposes we show in Figs. 1–6 x-y plot of the electronic density of these NO's as well as their average between the two Σ states. In all these figures the molecule lies in the z axis, the copper atom on the left. Note that the second highest occupied MAO (second HOMAO, Fig. 3) is almost identical to the highest occupied natural orbital (HONO) of the ground state (Fig. 1), whereas the HOMAO (Fig. 4) comes mainly from the HONO of the excited state (Fig. 6).

V. CONCLUSION

The estimation of radiative lifetimes imposes two serious demands that must be fulfilled in order to obtain accurate values, namely, good enough transition energies and dipole moments. Nevertheless, lifetimes are significantly more sensitive to variations in the transition dipole moments than they are to energy differences. This could be easily observed in the case of the Σ excited state.

In order to properly calculate transition dipole moments in orthogonal basis sets one needs a reasonably good one-electron basis to describe both the initial and final states involved in the electronic transition. We proposed here an alternative and inexpensive way to obtain monoelectronic basis sets that describe with nearly the same quality the initial and final states. We tested our method in the case where both states belong to the same or to a different molecular symmetry. The dramatic improvement of the calculated transition dipole moments, either using the zeroth- or the first-order MAO's, leads us to values that are in very good agreement with recent experimental data.

Finally, we can say that the differences between the transition dipole moments calculated using the MAO's obtained through the zeroth- or first-order arithmetic mean of the spinless one-particle reduced density matrices ($\bar{G}^{(0)}$ or $\bar{G}^{(1)}$) are indeed very small and therefore the additional computational effort to obtain the first-order MAO's is no longer justified.

ACKNOWLEDGMENTS

One of us (A.R.S.) would like to thank the Universidad Nacional Autónoma de México (Instituto de Física) for support at the Laboratoire de Physique Quantique de Toulouse and Dr. F. Spiegelmann and for many illuminating talks. We also acknowledge interesting discussions with Professor J. Schamps, who suggested to us the study of the CuX family. The Laboratoire de Physique Quantique is "Laboratoire associée (no. 505) du Centre National de la Recherche Scientifique."

[1]C. Dufour, J. Schamps, and R. F. Barrow, J. Phys. B **15**, 3819 (1982).
[2]J. M. Delaval, J. Schamps, and Y. Lefebvre, Chem. Phys. Lett. **115**, 378 (1985).
[3]J. M. Delaval and J. Schamps, Chem. Phys. **100**, 21 (1985).
[4]N. W. Winter and D. L. Huestis, Chem. Phys. Lett. **133**, 311 (1987).
[5]M. T. Nguyen, M. A. McGuinn, and N. J. Fitzpatrick, J. Chem. Soc. Faraday Trans. **82**, 1427 (1986).
[6]A. Ramírez-Solís and J. P. Daudey, Chem. Phys. **134**, 111 (1989).
[7]A. Ramírez-Solís and J. P. Daudey, J. Phys. B **23**, 2277 (1990).
[8]S. B. Rai and D. K. Rai, Chem. Phys. Lett. **80**, 606 (1981).
[9]K. P. R. Nair, Chem. Phys. Lett. **92**, 271 (1982).
[10]W. J. Balfour and R. S. Ram, J. Phys. B **17**, 219 (1984).
[11]J. M. Delaval, Y. Lefebvre, H. Boquet, P. Bernage, and P. Niay, Chem. Phys. **111**, 129 (1987).
[12]F. Ahmed, R. F. Barrow, A. H. Chojnicki, C. Dufour, and J. Schamps, J. Phys. B **15**, 3801 (1982).
[13]P. Baltayan, F. Hartmann, J. C. Pebay-Peyroula, and N. Sadeghi, Chem. Phys. **120**, 123 (1988).
[14]P. Baltayan, F. Hartmann, I. Hikmet, J. C. Pebay-Peyroula, and N. Sadeghi, Chem. Phys. Lett. **160**, 549 (1989).
[15]P. E. Steele and H. P. Broida, J. Chem. Phys. **69**, 2300 (1978).
[16]Ph. Durand and J. C. Barthelat, Theoret. Chim. Acta **38**, 283 (1975); J. C. Barthelat, Ph. Durand, and A. Serafini, Mol. Phys. **33**, 179 (1979); J. C. Barthelat, and Ph. Durand, Gazz. Chim. Ital. **108**, 255 (1978).
[17]M. Pélissier, J. Chem. Phys. **75**, 775 (1981).
[18]Y. Bouteiller, C. Mijoule, M. Nizam, J. C. Barthelat, J. P. Daudey, M. Pélissier, and B. Silvi, Mol. Phys. **65**, 295 (1988).
[19]B. Huron, P. Rancurel, and J. P. Malrieu, J. Chem. Phys. **58**, 5745 (1973); S. Evangelisti, J. P. Daudey, and J. P. Malrieu, Chem. Phys. **75**, 91 (1983).